Published in final edited form as:
J Comp Neurol. 2014 August 1; 522(11): 2594–2608. doi:10.1002/cne.23551.

A Unique Ion Channel Clustering Domain on the Axon Initial Segment of Mammalian Neurons

Anna N. King[1], **Colleen F. Manning**[1], and **James S. Trimmer**[1,2]

[1]Department of Neurobiology, Physiology and Behavior, University of California, Davis, CA 95616

[2]Department of Physiology and Membrane Biology, University of California, Davis, CA 95616

Abstract

The axon initial segment (AIS) plays a key role in initiation of action potentials and neuronal output. The plasma membrane of the AIS contains high densities of voltage-gated ion channels required for these electrical events, and much recent work has focused on defining the mechanisms for generating and maintaining this unique neuronal plasma membrane domain. The Kv2.1 voltage-gated potassium channel is abundantly present in large clusters on the soma and proximal dendrites of mammalian brain neurons. Kv2.1 is also a component of the ion channel repertoire at the AIS. Here we show that Kv2.1 clusters on the AIS of brain neurons across diverse mammalian species including humans define a non-canonical ion channel clustering domain deficient in Ankyrin-G. The sites of Kv2.1 clustering on the AIS are sites where cisternal organelles, specialized intracellular calcium release membranes, come into close apposition with the plasma membrane, and are also sites of clustering of GABAergic synapses. Using an antibody specific for a single Kv2.1 phosphorylation site, we find that the phosphorylation state differs between Kv2.1 clusters on the proximal and distal portions of the AIS. Together, these studies show that the sites of Kv2.1 clustering on the AIS represent specialized domains containing components of diverse neuronal signaling pathways that may contribute to local regulation of Kv2.1 function and AIS membrane excitability.

Keywords

potassium channel; localization; immunohistochemistry; cisternal organelle; phosphorylation

Introduction

The axon initial segment (AIS) is a structurally and functionally specialized region of axons that plays diverse roles in neuronal biology as the site of action potential initiation (Clark et

Address correspondence to James S. Trimmer, PhD, Department of Neurobiology, Physiology and Behavior, 196 Briggs Hall, University of California, One Shields Avenue, Davis, CA 95616-8519. jtrimmer@ucdavis.edu.

Role of authors: All authors had full access to all the data in the study and take responsibility for the integrity of the data and the accuracy of the data analysis. Study concept and design: ANK, CFM, JST. Acquisition of data: ANK, JST. Analysis and interpretation of data: ANK, CFM, JST. Drafting of the manuscript: ANK, JST. Critical revision of the manuscript for important intellectual content: ANK, CFM, JST. Statistical analysis: ANK, CFM. Obtained funding: JST. Administrative, technical, and material support: JST. Study supervision: JST.

Conflict of interest. The authors declare no competing financial interests.

al., 2009), the major determinant of polarity (Szu-Yu Ho and Rasband, 2011), and as a protein and lipid diffusion barrier (Winckler et al., 1999; Song et al., 2009). The AIS has a specialized molecular composition to execute these unique functions (Grubb and Burrone, 2010; Rasband, 2011; Kole and Stuart, 2012). A distinct repertoire of voltage-gated ion channels is present on the AIS (Bender and Trussell, 2012). Voltage-gated sodium (Nav) channels on the AIS mediate the rapid depolarizing phase of action potentials, and AIS voltage-gated potassium (Kv) channels play critical roles in action potential repolarization, and in setting action potential threshold, interspike interval and firing frequency (Kole and Stuart, 2012). Specific forms of Nav and Kv channels are present at high densities in specific AIS subdomains (Van Wart et al., 2007; Lorincz and Nusser, 2008) due to interactions with scaffolding molecules such as Ankyrin-G (AnkG; for Nav and Kv7 channels), and PSD-93 (Kv1 channels), reviewed in (Vacher and Trimmer, 2012). Intracellular Ca^{2+} release channels present in cisternal organelles (Kosaka, 1980), and ionotropic GABAergic synapses (Benedeczky et al., 1994), also have highly restricted localizations within the AIS.

While many aspects of AIS structure and function are fundamental to neurons in varied vertebrate species (Hill et al., 2008), there exists substantial diversity between different types of mammalian neurons (Lorincz and Nusser, 2008). Moreover, there is plasticity in AIS structure and function (Grubb et al., 2011), in that dynamic changes in expression, localization and function of AIS ion channels through activity-dependent signaling pathways underlies modulation of neuronal network activity (Grubb et al., 2011). The AIS is also a “hotspot’ for epileptogenesis, as many ion channel subunits mutated in epilepsy are localized to the AIS (Wimmer et al., 2010).

The Kv2.1 channel is unusual for its robust expression in large clusters on the soma and proximal dendrites (Trimmer, 1991; Lim et al., 2000), and its extensive posttranslational modification (Cerda et al., 2011). Kv2.1 undergoes rapid activity-dependent regulation by reversible changes in these modifications, including phosphorylation at up to 34 sites (Misonou et al., 2006; Park et al., 2006; Trimmer and Misonou, 2014) and SUMOylation (Plant et al., 2011). While somatodendritic Kv2.1 clusters are seen in neurons throughout the nervous system of diverse species, in response to enhanced neuronal activity Kv2.1 is subjected to calcineurin-dependent dephosphorylation resulting in a loss of clustering and changes in channel gating that yield enhanced channel activity (Misonou et al., 2004; Misonou et al., 2006). The dynamic activity-dependent modulation of Kv2.1 acts to homeostatically regulate intrinsic neuronal excitability (Misonou et al., 2006; Mohapatra et al., 2009). A subpopulation of Kv2.1 channels is also clustered on the AIS (Sarmiere et al., 2008), although their molecular characteristics and regulation have not been investigated. Here we find that sites of Kv2.1 clustering on the AIS define a unique non-canonical AnkG-deficient ion channel-clustering domain that also contains other signaling proteins crucial to AIS function, and that may contribute to modulation of Kv2.1 channels on the AIS by activity-dependent changes in phosphorylation state.

Materials and Methods

Preparation of brain sections

This study was approved by the UC Davis Institutional Animal Care and Use Committee, and the Institutional Review Board and conforms to guidelines established by the NIH. Rats and mice were deeply anesthetized with 60 mg/kg sodium pentobarbital and perfused through the ascending aorta with phosphate buffered saline, pH7.4, and 4% formaldehyde, prepared from freshly depolymerized paraformaldehyde, in 0.1 M sodium phosphate buffer (PB), pH 7.4. The brains were removed, cryoprotected for 18 hr in 10% sucrose, then 48 hr in 30% sucrose. All samples of wild-type and *Kv2.1*$^{-/-}$(Jacobson et al., 2007) mouse brains were obtained from littermates from heterozygotic crosses. Perfusion fixed and cryoprotected macaque monkey and ferret brains were gifts from the laboratories of our late colleagues Dr. Edward G. Jones and Dr. Barbara Chapman, respectively. Fresh frozen human brain samples (49.5 year old Caucasian male, 5 hour postmortem interval) were obtained from the NICHD Brain and Tissue Bank for Developmental Disorders and NICHD Contract #HHSN275200900011C, Ref. No. NO1-HD-9-0011. Samples from frontal cortex were thawed in 4% formaldehyde, prepared from freshly depolymerized paraformaldehyde, in 0.1 M sodium phosphate buffer (PB), pH 7.4, and fixed for 30 min. at 4°C, cryoprotected for 18 hr in 10% sucrose, then 48 hr in 30% sucrose. Following cryoprotection, all samples were frozen, and cut into 40 μm sections on a freezing stage sliding microtome. Sections were collected in 0.1 M PB and processed immediately for immunohistochemistry.

Acute seizures were induced in adult male rats by systemic kainate administration at a dose of 10 mg/kg (Misonou et al., 2004). Seizure progression was assessed by visual observation of the behavioral seizure stage according to Racine's classification (Racine et al., 1972). A full tonic-clonic behavioral seizure, with loss of postural control, was considered as a class 5 motor seizure. Animals that had a class 5 seizure were anesthetized with pentobarbital and perfused as described above. Hypoxia was induced in rats that had been anesthetized with pentobarbital by exposure to 100% CO_2 for 2 minutes (Misonou et al., 2005), which yield effects on Kv2.1 phosphorylation similar to that obtained with other hypoxia models (Ito et al., 2010) followed by perfusion as described above.

Antibody characterization

Table 1 contains a list of antibodies and dyes used in this study. We refer the reader to the JCN antibody database (http://onlinelibrary.wiley.com/journal/10.1002/(ISSN)1096-9861/homepage/jcn_antibody_database.htm) for details on mouse monoclonal antibodies against Kv2.1 (K89/34, NeuroMab), Ankyrin-G (N106/36, NeuroMab), Kv1.2 (K14/16, NeuroMab), ryanodine receptor (34C, Pierce), Gephyrin (mAb7a, Synaptic Systems) and rabbit polyclonal antibodies against VGAT (Synaptic Systems). Trimmer lab anti-Kv2.1 rabbit polyclonal antibodies KC and pS603 were previously validated by immunoblots against Kv2.1 KO mouse brain samples (Misonou et al., 2006). NeuroMab mouse monoclonal antibodies were validated as follows: anti-Ankyrin-G N106/65: reactivity against AnkG and lack of cross reactivity against Ankyrin B in heterologous cells. N106/65 does not recognize denatured Ankyrin-G on immunoblots, but has an identical pattern of staining in brain sections (*i.e.*, specific labeling of nodes of Ranvier and the AIS) as clone

N106/36. N106/36 yields a single band of the appropriate size on immunoblots of rat and mouse brain samples, reactivity against AnkG and lack of cross reactivity against Ankyrin B in heterologous cells, and is in the JCN antibody database; Anti-Nav1.6 K87A/10: does not recognize denatured Nav1.6 on immunoblots, but yields specific labeling of nodes of Ranvier and the AIS in brain sections, and labels cerebellar granule cells cultured from wild-type mice but not those cultured from Nav1.6 null mice; anti-GABA-A α1 receptor N95/35: yields a single band of expected size (52 kD) on immunoblots of rat and mouse brain samples, this band is not seen in a similar sample prepared from GABA-A α1 receptor KO mice; anti-GABA-A β1 receptor N96/55: yields a single band of expected size (55 kD) on immunoblots of rat brain samples, does not cross-react with GABA-A β2 receptor or GABA-A β3 receptor in heterologous cells; anti-GABA-A β3 receptor N87/25: yields a single band of expected size (55 kD) on immunoblots of rat, mouse and human brain samples, does not cross-react with GABA-A β1 receptor or GABA-A β2 receptor in heterologous cells. Anti-synaptopodin mouse monoclonal antibody G1D4 (Acris) was generated against podocytes and was originally characterized as yielding a single 44 kD band on immunoblots of kidney, and as labeling podocyte foot processes (Mundel et al., 1991). This mouse monoclonal antibody yields labeling in podocytes and brain identical to the rabbit polyclonal antibody validated by synaptopodin KO mouse experiments (Deller et al., 2003), including labeling of CO-associated puncta on the AIS that is eliminated in synaptopodin KO mice (Bas Orth et al., 2007); Anti-α-actinin mouse monoclonal antibody EA-53 (Sigma) labels a single band of the expected size (100 kD) on immunoblots of rat brain (Wyszynski et al., 1998).

Multiple immunofluorescence labeling

Multiple immunofluorescence labeling was performed essentially as described (Manning et al., 2012). In brief, sections were first rinsed in PB. Free-floating sections were incubated in 10% v/v goat serum in PB containing 0.3% v/v Triton X-100 (vehicle) for 1 h and then incubated overnight at 4°C in vehicle containing different combinations of primary antibodies. Following overnight incubation in primary antibodies, sections were washed 3X for 10 min each in vehicle, and incubated for 1 h in vehicle containing affinity-purified species and/or mouse IgG-subclass-specific goat secondary antibodies conjugated to Alexa fluors (Life Technologies). Sections were labeled with dyes (Hoechst 33258, phallacidin) during the secondary antibody step. Sections were washed in 0.1M PB, dried, and cover-slipped using ProLong Gold mounting medium (Life Technologies).

Unless otherwise noted, all images were obtained on a Zeiss AxioObserver Z1 microscope (Carl Zeiss MicroImaging) equipped with an AxioCam HRm high resolution monochromatic digital camera and an Apotome structured illumination system, using a 100X plan-Neofluar 1.3 NA oil immersion objective. Imaging and post-imaging processing was performed in Axiovision (Carl Zeiss MicroImaging), including line histograms of fluorescence intensity.

Confocal microscopy was performed at the UC Davis MCB LM Imaging Facility, on an Olympus FV1000 Laser Scanning Confocal microscope. Super-resolution structured illumination microscopy was performed on two microscopes based on the structured

illumination technique (Gustafsson et al., 2008). Nokia 3D-SIM analyses was performed at the UC Davis MCB LM Imaging Facility using a Nikon Eclipse Ti microscope fitted with a Apo TIRF 100x/1.48 oil objective and 488 nm and 561 nm lasers. Capture and post capture image processing was done using Nokia NIS-Elements AR imaging software v4.11. Super-resolution light microscopy was also performed on a Zeiss Elyra SIM microscope, and equipped with a Plan Apochromat 100X/1.46 NA oil immersion objective and 488 nm and 561 nm lasers, in conjunction with Carl Zeiss MicroImaging and specialist Bryant Chhun.

Linear adjustments to contrast and brightness were performed using Photoshop (Adobe Systems). All panels in given figure were imaged and treated identically. The contrast and brightness of the magnified insets were adjusted to highlight spatial expression patterns of individual target molecules.

Results

Kv2.1 is clustered at specific AnkG–deficient sites on the AIS of neocortical pyramidal cells

The Kv2.1 voltage-gated potassium channel exhibits robust expression in large clusters in neuronal somata and proximal dendrites in most mammalian central neurons (Trimmer, 1991; Lim et al., 2000) (Fig. 1). A recent study revealed that in addition to this prominent somatodendritic localization, a subpopulation of Kv2.1 is also present on the AIS of rat hippocampal neurons in culture, and in rat brain, in neurons in CA1-CA3 layers of hippocampus, and layer IV of neocortex (Sarmiere et al., 2008). Figure 1 reveals that the clustered localization of Kv2.1 on the AIS is also seen in mouse neocortex. This labeling, while difficult to see amidst the extensive Kv2.1 labeling (green) on neuronal somata and proximal dendrites (Fig. 1A), is revealed upon double labeling with the AIS marker AnkG (red, Fig. 1B). That this labeling is specific for Kv2.1 is supported by its presence with multiple anti-Kv2.1 antibodies (data not shown), and by the loss of this labeling in sections prepared from *Kv2.1*$^{-/-}$ (Kv2.1 KO) mice that were labeled and imaged identically as the sections from WT littermates (Fig. 1D).

We found that the labeling for clustered Kv2.1 (green) on the AIS is mutually exclusive with that for AnkG (red, Fig. 2). Images obtained with a Zeiss Elyra super resolution structured illumination microscope (Fig. 2A-F) reveal that the Kv2.1 clusters reside at AIS sites that are located primarily over “holes” in the AnkG scaffold. A similar contrasting distribution of Kv2.1 and AnkG is observed in images from multiple distinct microscope systems, including a Zeiss Apotome structured illumination system (Fig. 2G,H,M,N), an Olympus scanning laser confocal microscope (Fig. 2I,J,O,P), and a Nikon N-SIM structured illumination system (Fig. 2K,L,Q,R). The histograms of line scans through the magnified insets in Fig. 2 highlight that the maxima of Kv2.1 labeling (green) are primarily located at/near the minima of AnkG labeling (red). Thus, the presence of Kv2.1 clusters at sites deficient in AnkG labeling is independent of the imaging technique used, and is not an artifact of imaging.

The observation that Kv2.1 clusters are primarily located at sites on the AIS lacking prominent AnkG labeling led us to question whether the Kv2.1 clusters themselves were

instructive in generating and/or maintaining this discontinuous distribution of AnkG. However, as shown in Fig. 1D, the non-uniform distribution of AnkG seen in brain sections from rats (Fig. 2) and WT mice (Fig. 1B-C) is also seen in brain sections from WT and *Kv2.1*$^{-/-}$ mouse littermates (Fig. 1D). This demonstrates that the presence of clustered Kv2.1 is not necessary for generating and maintaining AnkG-deficient sites on the AIS.

The localization of Kv2.1 at AnkG-deficient sites on the AIS is seen in different brain regions

We next determined whether the contrasting localization of Kv2.1 and AnkG observed in neocortical neurons is seen in other neurons in rat brain. In CA1 pyramidal neurons, we observe small clusters of Kv2.1 (green), primarily at AnkG (red)-deficient sites along the AIS (Fig. 3A,H). Kv2.1 is expressed in both parvalbumin-positive and parvalbumin-negative interneurons in hippocampus (Du et al., 1998). We find Kv2.1 predominantly at AnkG-deficient sites on the AIS of both classes of interneurons in *stratum oriens* of CA1 (Positive: Fig. 3B,I; Negative Fig. 3C,J). Dentate granule cells also express clustered Kv2.1 at AnkG-deficient sites on the AIS (Fig. 3D,K). Neurons in posterior nucleus (Fig. 3E,L) and lateral posterior nucleus (Fig. 3F,M) of the thalamus also exhibit the mutually exclusive localization of Kv2.1 and AnkG. Finally, medium spiny neurons, the major output neurons of the striatum, also have clustered Kv2.1 on the AIS (Fig. 3G,N), where it is again found at AnkG-deficient sites. Together, these findings suggest that the localization of Kv2.1 clusters at AnkG-deficient sites on the AIS is seen on diverse rat brain neurons.

Localization of Kv2.1 to AnkG-deficient sites on the AIS is seen in diverse mammalian species

The localization of Kv2.1 clusters at AnkG-deficient sites on the AIS in rat and mouse brain led us to question whether this localization was specific to rodents or is present in other mammalian species. We performed double labeling for Kv2.1 and AnkG in samples from representatives from order Carnivora (ferret), a non-human primate (rhesus macaque monkey), and human. Samples of ferret and macaque brain were prepared from perfusion fixed specimens, while human samples were from fresh frozen post-mortem brains that were sectioned and then post-fixed.

The overall localization of Kv2.1 in large clusters on neuronal somata and proximal dendrites, as previously described in rat brain (Trimmer, 1991; Hwang et al., 1993; Scannevin et al., 1996), is observed in these species (data not shown). Figure 4 shows examples of the AIS of layer 5 cortical pyramidal neurons double labeled for Kv2.1 (green) and AnkG (red). Analyses of the AIS in rat (Fig. 4A,F), ferret (Fig. 4B,G), macaque monkey (Fig. 4C,H) and human (Fig. 4D,E,I,J) brain revealed that Kv2.1 on the AIS clusters primarily at AnkG-deficient sites in each of these species. These data suggest a conserved role for Kv2.1 clustering at AnkG-deficient sites on the AIS across disparate mammalian species.

Kv2.1 clusters define a unique AIS ion channel-clustering domain

Nav and Kv1 channels are present at high levels in distinct domains in the AIS (Van Wart et al., 2007; Lorincz and Nusser, 2008). To determine the relationship of the restricted

subcellular distribution of AIS Kv2.1 clusters to other voltage-gated ion channels on the AIS, we analyzed the distribution of Nav1.6 and Kv1.2 α subunits in the AIS of neocortical pyramidal cells. Triple labeling in neocortical layer V pyramidal cells reveals intense immunolabeling for Nav1.6 (red); this immunolabeling colocalized prominently with AnkG (blue) in more distal portions of the AIS (Fig. 5A,B,E,F). Nav1.6 is excluded from the sites of Kv2.1 (green) clustering, consistent with the lack of AnkG at these sites. A similar overlapping distribution of Nav1.6 and AnkG, and their mutually exclusive relationship to Kv2.1 clusters, is also found in hippocampal CA1 pyramidal neurons (data not shown).

Kv1 channels are also widely expressed at the AIS, where they exhibit overlap with Nav1.6 and AnkG, and are more prominent in distal than proximal regions of the AIS (Van Wart et al., 2007; Lorincz and Nusser, 2008). We found immunolabeling for Kv1.2 (red) generally overlapping with AnkG labeling (blue), and excluded from regions containing Kv2.1 (green) clusters, in a pattern somewhat similar to Nav1.6((Fig. 5C,D,G,H). This mutually exclusive distribution of Kv2.1 and Kv1 channels is also present in hippocampal CA1 pyramidal cells (data not shown).

Kv2.1 clusters are present in proximal regions of the AIS lacking Nav1.6, and Kv1.2 labeling (Fig. 5). However, the clusters of Kv2.1 do not extend past the distal boundary of the AnkG labeling (*i.e.*, into the axon proper). This pattern of Kv2.1 localization along the entire AIS, and the mutual exclusion with these other ion channels in the distal AIS, is observed in all classes of neurons examined in rat and mouse brain. Overall, these results suggest a mosaic of ion channel expression on the AIS, with distinct membrane subdomains of Nav1.6 and Kv1.2, and of clustered Kv2.1.

Kv2.1 AIS clusters are located at sites near cisternal organelles

The distinctive localization of Kv2.1 clusters, and their lack of overlap with AnkG and other voltage-gated ion channels, raised questions as to whether any other AIS proteins were present at sites of Kv2.1 clustering. Cisternal organelles (COs) are smooth endoplasmic reticulum that runs along the core of the axon, and that comes into close apposition to the plasma membrane at specific AIS sites (Benedeczky et al., 1994). Triple immunolabeling of rat neocortical layer 5 pyramidal cells for Kv2.1 (green), AnkG (blue) and the cisternal organelle (CO) marker synaptopodin (red) (Bas Orth et al., 2007) revealed that Kv2.1 clusters were consistently localized adjacent to, but not overlapping with, synaptopodin clusters (Fig. 6A,G). Triple immunolabeling for Kv2.1, AnkG and ryanodine receptors (RyR, red), an intracellular calcium release channel in the CO membrane, showed a similar relationship (Fig. 6B,H). COs contain a set of actin-associated cytoskeletal elements, including the actin binding protein α-actinin. Puncta of α-actinin (red) are also found adjacent to, but not overlapping with, Kv2.1 clusters (green) at AIS sites deficient in AnkG (Fig. 6C,I). This is consistent with the previously described colocalization of synaptopodin and α-actinin within the AIS of neocortical neurons (Sanchez-Ponce et al., 2012). Patches of F-actin are also present on the AIS (Watanabe et al., 2012), and we found (Fig. 6D,J) that clusters of Kv2.1 (green) are often found adjacent to these F-actin patches (red).

As expected for a plasma membrane ion channel, the clusters of Kv2.1 do not completely overlap the high-density puncta of intracellular synaptopodin and RyR, or α-actinin and F-

actin patches. Moreover, synaptopodin and α-actinin clusters often appear rod-shaped and more elongated than do Kv2.1 clusters. In some cases, two distinct Kv2.1 clusters localize to one α-actinin or synaptopodin cluster. Given the relationship of clusters of Kv2.1 and COs, we next determined whether the presence of Kv2.1 clusters was required for the generation and maintenance of the specific sites where the cisternal organelles come into close apposition to the plasma membrane. We compared labeling for synaptopodin (Fig. 6) in WT mice (Fig. 6E,K), and in their *Kv2.1*$^{-/-}$ littermates (Fig. 6F,L), and found no obvious difference in expression and localization of synaptopodin or any of the other CO markers examined here (data not shown). This suggests that the presence of Kv2.1 clusters at these sites is not necessary for directing the localization of COs.

Kv2.1 clusters on the AIS are located near GABA-A synapses

We next used triple labeling to determine whether Kv2.1 clusters were located near GABA-A receptor containing synapses on the AIS. We found that punctate labeling for postsynaptic α1 (Fig. 7A,F), β1 (Fig. 7B,G), and β3 (Fig. 7C,H) GABA-A receptor subunits (red) on the AIS (as marked by blue AnkG labeling) was often found clustered near Kv2.1 (green) clusters. The GABA-A receptor scaffolding protein gephryin (red) was also found adjacent to, but not colocalized with, Kv2.1 (green) clusters, near the edges of the AnkG-deficient regions of the AIS (Fig. 7D,I). Note that the labeling for the smaller GABA-A receptor subunit and gephyrin puncta was often adjacent to, but not colocalized with, labeling for the larger Kv2.1 clusters. In contrast to Kv2.1 labeling, which was centrally localized at AnkG deficient sites or holes, labeling for the postsynaptic components of the GABA-A synapses are primarily located at the periphery of the AnkG (blue) holes (Fig. 7). Labeling for VGAT (red), a marker for GABAergic presynaptic terminals, was also found associated with Kv2.1 (green) clusters (Fig. 7E,J). However, VGAT labeling was superficial to and did not overlap the Kv2.1 labeling on the AIS itself, as expected for nerve endings displaced physically opposed to their postsynaptic targets.

AIS and somatodendritic Kv2.1 exhibit distinct patterns of phosphorylation and clustering regulation

We used labeling with a phosphospecific antibody against the pS603 phosphorylation site of Kv2.1 (red) to gain insights into the phosphorylation state of the subpopulation of Kv2.1 (green) on the AIS (marked by AnkG in blue) relative to the more prominent somatodendritic pool of Kv2.1. As shown in Fig. 8, the subpopulation of Kv2.1 on the proximal AIS in control animals (top arrows in Fig. 8 panels F,G,I; panels K, L, N) exhibits a pattern of phosphorylation broadly similar to the somatodendritic pool. However, the clusters of Kv2.1 on the more distal portions of the AIS (bottom arrows in Fig. 8 panels F,G,I; panels P,Q,S) did not exhibit phosphospecific antibody labeling. This suggests that, similar to the differences in the expression pattern of other AIS ion channels (*e.g.*, the Nav1.6 and Kv1.2 labeling shown in Fig. 5), the proximal and distal regions of AIS are also distinct in maintaining Kv2.1 in distinct phosphorylation states.

We next determined how phosphorylation of the pool of Kv2.1 on the AIS was regulated by two stimuli known to trigger dephosphorylation of somatodendritic Kv2.1: *status epilepticus* induced by systemic exposure to kainate (Misonou et al., 2004; Misonou et al., 2006), and

brief CO_2 exposure (Misonou et al., 2005), which induces effects on Kv2.1 phosphorylation similar to other models of hypoxia (Misonou et al., 2005; Ito et al., 2010). We observe a loss of phosphospecific antibody labeling of both the somatic and proximal AIS Kv2.1 in animals subjected to these treatments (Fig. 8, kainate: panels C,H,M,R; CO_2: panels E,J,O,T). However, in neurons in which the somatodendritic Kv2.1 pool has lost its clustering in response to these stimuli, Kv2.1 on the AIS remains clustered (Fig. 8). These data suggest the presence of diverse patterns of phosphorylation-dependent regulation of Kv2.1 in distinct neuronal compartments, and between the proximal and distal subdomains of the AIS.

Discussion

Here we show that Kv2.1 clusters are present on the AIS at sites deficient in AnkG in diverse neuronal types within rat brain, and across diverse mammalian species. We also show that the sites of Kv2.1 clustering contain an array of proteins involved in diverse neuronal signaling pathways, and that the Kv2.1 clustered at these unique AIS sites exhibits spatially distinct patterns of phosphorylation.

AnkG is the master organizer of the AIS (Hedstrom et al., 2008; Sobotzik et al., 2009; Galiano et al., 2012), and through direct binding plays a crucial role in clustering specific AIS ion channels, including Nav channels (Jenkins and Bennett, 2001; Brachet et al., 2010) and Kv7 potassium channels (Pan et al., 2006; Rasmussen et al., 2007), which contain specific AnkG binding motifs (Garrido et al., 2003; Lemaillet et al., 2003). Here we define an AnkG-deficient subdomain of the AIS that is the site of Kv2.1 clustering, and is enriched in components of COs and GABAergic synapses (Fig. 9). AnkG-deficient sites in the AIS are apparent in published images [e.g., (Xiao et al., 2013)] but a specific association of these sites with other elements of the AIS, including specific ion channels and signaling molecules, has not been elucidated. We speculate that the gaps in the dense AnkG-spectrin-actin scaffolding system at these AnkG-deficient sites are needed to accommodate the high density of protein complexes containing plasma Kv2.1 channels, GABA-A receptor-containing synapses, and to allow the intracellular membranes associated with the CO to come in close apposition to the plasma membrane (Fig. 9). The sites of Kv2.1 clustering on the AIS may be related to the membrane subdomain bounded by an actin-associated perimeter fence that has been proposed to contribute to Kv2.1 clustering (O'Connell et al., 2006; Tamkun et al., 2007).

Previous studies have revealed that the canonical AnkG-based ion channel clustering system appeared early in chordate evolution (Hill et al., 2008). The AnkG-based ion channel clustering system for Nav channels is present in the lamprey (Hill et al., 2008), separated from the human lineage by ≈535 million years (Hedges et al., 2006). Other components of the AIS ion channel repertoire anchored by AnkG, such as Kv7 channels, appeared later in evolution (Hill et al., 2008). Here we show that the presence of Kv2.1 clusters at AnkG-deficient sites on the AIS is highly conserved across diverse mammalian species that together represent 94 million years of evolutionary divergence (Hedges et al., 2006).

Specific voltage-gated ion channels exhibit compartmentalized expression in distinct microdomains within the AIS. Studies on the AIS of retinal ganglion cells revealed that Nav1.1 and Nav1.6 were preferentially localized to proximal and distal regions of the AIS, respectively (Van Wart et al., 2007). Subsequent studies revealed that distinct types of mammalian brain neurons exhibit diversity in the molecular composition of the ion channel repertoire in the AIS, including expression of Nav1.1 or Nav1.2 as the predominant proximal AIS Nav isoforms, and Nav1.6 as the distal isoform (Lorincz and Nusser, 2008; Hu et al., 2009; Duflocq et al., 2011). Kv channels also exhibit distinct localization within the AIS, with Kv7 channels located in the proximal AIS (Klinger et al., 2011), and Kv1 channels at the distal AIS (Van Wart et al., 2007; Lorincz and Nusser, 2008; Ogawa et al., 2008). The highly organized patterns of expression of specific ion channels in subdomains of the AIS underlies the specific properties of action potential initiation (Kole and Stuart, 2012).

While the proximal and distal populations of Kv2.1 exhibit similar properties in their association with components of COs and GABA-A receptor macromolecular assemblies at these AnkG-deficient sites in layer 5 neocortical pyramidal neurons, these Kv2.1 populations differ in regulation of their phosphorylation state. For at least one phosphorylation site (S603) that has been shown to impact Kv2.1 function (Misonou et al., 2006; Park et al., 2006), the proximal Kv2.1 clusters are maintained in a phosphorylation state similar to that observed on the soma and proximal dendrites, while those on the distal AIS are maintained in distinct state. While the phosphorylation state of somatodendritic Kv2.1, and of the Kv2.1 on the proximal AIS, are coordinately regulated in an activity-dependent manner in response to acute seizures and hypoxia, the clustering of Kv2.1 is not, suggesting that phosphorylation-dependent regulation of Kv2.1 clustering and gating is also distinct between the somatodendritic compartment and the AIS.

The localization of Kv2.1 near sites of intracellular calcium release from COs is intriguing, given that the Ca^{2+}/calmodulin-dependent protein phosphatase calcineurin plays a key role in the activity-dependent regulation of Kv2.1 phosphorylation state (Misonou et al., 2004; Misonou et al., 2006; Park et al., 2006). Recent studies in cultured dentate granule cells revealed that while calcineurin is not enriched in the AIS, it plays a critical role in activity-dependent changes in the location of the AIS (Evans et al., 2013). The Ca^{2+}-dependent protease calpain mediates disruption of the AIS following brain injury (Schafer et al., 2009). The source of Ca^{2+} in these events that modify AIS structure is not known. However, the localization of Kv2.1 and GABA-A receptors, which are modulated by Ca^{2+}-dependent signaling pathways acting through CamKII (Saliba et al., 2012) and calcineurin (Dacher et al., 2013), near sites of intracellular Ca^{2+} release on the AIS provides a possible machinery for their efficient modulation. Kv2.1 is located near structures analogous to the CO on the somatodendritic domain of hippocampal CA1 pyramidal neurons (Du et al., 1998), and knockdown of Kv2.1 leads to altered Ca^{2+} signaling in these cells (Du et al., 2000). As such it is possible that the localization of Kv2.1 on the AIS at sites adjacent to COs may reciprocally impact Ca^{2+} signaling in these domains, through local effects on membrane potential and plasma membrane Ca^{2+} entry pathways. Elements of the CO are also associated with the spine apparatus of dendritic spines. Proteins associated with the CO, especially synaptopodin (Vlachos et al., 2009; Vlachos et al., 2013; Zhang et al., 2013), are

crucial to the formation of the spine apparatus (Deller et al., 2003) and to the RyR-mediated intracellular Ca^{2+} release that underlies certain forms of synaptic potentiation (Bardo et al., 2006; Deller et al., 2007). We speculate that the CO may play an analogous role in Ca^{2+}-dependent plasticity of the AIS, including through Ca^{2+}/calcineurin-dependent modulation of Kv2.1.

Previous immunogold electron microscopy labeling of Kv2.1 on somata of CA1 pyramidal neurons established that Kv2.1 clusters are also located near symmetrical (i.e., GABAergic) synapses (Du et al., 1998). The Kv2.1 gold particles were not found within the synapse itself, but were found to flank the faint PSD. The light microscopic multiple labeling presented here reveals that Kv2.1 has a somewhat similar relationship with the axo-axonal GABAergic synapses present on the AIS, in that Kv2.1 labeling is found adjacent to, but not overlapping with, labeling for GABA-A receptor subunits and gephyrin on the AIS. In general, the Kv2.1 clusters appear to be more central to the AnkG “holes”, while the GABA-A receptor subunits and gephyrin are located more at the periphery of the holes (Fig. 9). This suggests that while the functions of the axo-somatic and axo-axonal GABAergic synapses may differ, and the inhibitory neurons that project onto these sites differ [*e.g.*, in neocortical pyramidal neurons, basket cells target the somata, and Chandelier cells the AIS; reviewed in (Woodruff et al., 2010)], the requirement for nearby Kv2.1 channels is shared. GABAergic synapses on the AIS have been proposed to be excitatory (Szabadics et al., 2006; Khirug et al., 2008). It is intriguing to speculate that Kv2.1 channels adjacent to these GABAergic synapses may mediate repolarization subsequent to an excitatory synaptic event, somewhat analogous to the coordinated action of excitatory Nav channels and inhibitory/repolarizing Kv1 and Kv7 channels in AnkG-rich domains of the AIS.

Supplementary Material

Refer to Web version on PubMed Central for supplementary material.

Acknowledgments

We thank Bryant Chhun (Carl Zeiss Microscopy, LLC) and Dr. Michael Paddy (UC Davis/MCB Imaging Facility) for assistance with Super-resolution imaging, and Hannah Bishop, Danielle Mandikian, and Dr. Karl Murray for suggestions and discussions. We are also grateful to our late colleagues Drs. Edward G. Jones and Barbara Chapman for providing monkey and ferret brains, respectively.

Funding: Supported by NIH grant R01 NS42225 (to JST).

References

Bardo S, Cavazzini MG, Emptage N. The role of the endoplasmic reticulum Ca2+ store in the plasticity of central neurons. Trends Pharmacol Sci. 2006; 27(2):78–84. [PubMed: 16412523]

Bas Orth C, Schultz C, Muller CM, Frotscher M, Deller T. Loss of the cisternal organelle in the axon initial segment of cortical neurons in synaptopodin-deficient mice. J Comp Neurol. 2007; 504(5): 441–449. [PubMed: 17701995]

Bender KJ, Trussell LO. The physiology of the axon initial segment. Ann Rev Neurosci. 2012; 35:249–265. [PubMed: 22443507]

Benedeczky I, Molnar E, Somogyi P. The cisternal organelle as a Ca(2+)-storing compartment associated with GABAergic synapses in the axon initial segment of hippocampal pyramidal neurones. Exp Brain Res. 1994; 101(2):216–230. [PubMed: 7843310]

Brachet A, Leterrier C, Irondelle M, Fache MP, Racine V, Sibarita JB, Choquet D, Dargent B. Ankyrin G restricts ion channel diffusion at the axonal initial segment before the establishment of the diffusion barrier. J Cell Biol. 2010; 191(2):383–395. [PubMed: 20956383]

Cerda O, Baek J, Trimmer J. Mining recent brain proteomic databases for ion channel phosphosite nuggets. J Gen Physiol. 2011; 137(1):3–16. [PubMed: 21149544]

Clark BD, Goldberg EM, Rudy B. Electrogenic tuning of the axon initial segment. Neuroscientist. 2009; 15(6):651–668. [PubMed: 20007821]

Dacher M, Gouty S, Dash S, Cox BM, Nugent FS. A-kinase anchoring protein-calcineurin signaling in long-term depression of GABAergic synapses. J Neurosci. 2013; 33(6):2650–2660. [PubMed: 23392692]

Deller T, Bas Orth C, Del Turco D, Vlachos A, Burbach GJ, Drakew A, Chabanis S, Korte M, Schwegler H, Haas CA, Frotscher M. A role for synaptopodin and the spine apparatus in hippocampal synaptic plasticity. Ann Anat. 2007; 189(1):5–16. [PubMed: 17319604]

Deller T, Korte M, Chabanis S, Drakew A, Schwegler H, Stefani GG, Zuniga A, Schwarz K, Bonhoeffer T, Zeller R, Frotscher M, Mundel P. Synaptopodin-deficient mice lack a spine apparatus and show deficits in synaptic plasticity. Proc Natl Acad Sci U S A. 2003; 100(18): 10494–10499. [PubMed: 12928494]

Du J, Haak LL, Phillips-Tansey E, Russell JT, McBain CJ. Frequency-dependent regulation of rat hippocampal somato-dendritic excitability by the K+ channel subunit Kv2.1. J Physiol. 2000; 522(Pt 1):19–31. [PubMed: 10618149]

Du J, Tao-Cheng JH, Zerfas P, McBain CJ. The K+ channel, Kv2.1, is apposed to astrocytic processes and is associated with inhibitory postsynaptic membranes in hippocampal and cortical principal neurons and inhibitory interneurons. Neuroscience. 1998; 84(1):37–48. [PubMed: 9522360]

Duflocq A, Chareyre F, Giovannini M, Couraud F, Davenne M. Characterization of the axon initial segment (AIS) of motor neurons and identification of a para-AIS and a juxtapara-AIS, organized by protein 4.1B. BMC Biology. 2011; 9:66. [PubMed: 21958379]

Evans MD, Sammons RP, Lebron S, Dumitrescu AS, Watkins TB, Uebele VN, Renger JJ, Grubb MS. Calcineurin signaling mediates activity-dependent relocation of the axon initial segment. J Neurosci. 2013; 33(16):6950–6963. [PubMed: 23595753]

Galiano MR, Jha S, Ho TS, Zhang C, Ogawa Y, Chang KJ, Stankewich MC, Mohler PJ, Rasband MN. A distal axonal cytoskeleton forms an intra-axonal boundary that controls axon initial segment assembly. Cell. 2012; 149(5):1125–1139. [PubMed: 22632975]

Garrido JJ, Giraud P, Carlier E, Fernandes F, Moussif A, Fache MP, Debanne D, Dargent B. A targeting motif involved in sodium channel clustering at the axonal initial segment. Science. 2003; 300(5628):2091–2094. [PubMed: 12829783]

Grubb MS, Burrone J. Building and maintaining the axon initial segment. Curr Opin Neurobiol. 2010; 20(4):481–488. [PubMed: 20537529]

Grubb MS, Shu Y, Kuba H, Rasband MN, Wimmer VC, Bender KJ. Short- and long-term plasticity at the axon initial segment. J Neurosci. 2011; 31(45):16049–16055. [PubMed: 22072655]

Gustafsson MG, Shao L, Carlton PM, Wang CJ, Golubovskaya IN, Cande WZ, Agard DA, Sedat JW. Three-dimensional resolution doubling in wide-field fluorescence microscopy by structured illumination. Biophys J. 2008; 94(12):4957–4970. [PubMed: 18326650]

Hedges SB, Dudley J, Kumar S. TimeTree: a public knowledge-base of divergence times among organisms. Bioinformatics. 2006; 22(23):2971–2972. [PubMed: 17021158]

Hedstrom KL, Ogawa Y, Rasband MN. AnkyrinG is required for maintenance of the axon initial segment and neuronal polarity. J Cell Biol. 2008; 183(4):635–640. [PubMed: 19001126]

Hill AS, Nishino A, Nakajo K, Zhang G, Fineman JR, Selzer ME, Okamura Y, Cooper EC. Ion channel clustering at the axon initial segment and node of Ranvier evolved sequentially in early chordates. PLoS Genetics. 2008; 4(12):e1000317. [PubMed: 19112491]

Hu W, Tian C, Li T, Yang M, Hou H, Shu Y. Distinct contributions of Na(v)1.6 and Na(v)1.2 in action potential initiation and backpropagation. Nat Neurosci. 2009; 12(8):996–1002. [PubMed: 19633666]

Hwang PM, Fotuhi M, Bredt DS, Cunningham AM, Snyder SH. Contrasting immunohistochemical localizations in rat brain of two novel K+ channels of the Shab subfamily. J Neurosci. 1993; 13(4): 1569–1576. [PubMed: 8463836]

Ito T, Nuriya M, Yasui M. Regulation of Kv2.1 phosphorylation in an animal model of anoxia. Neurobiol Dis. 2010; 38(1):85–91. [PubMed: 20079839]

Jacobson DA, Kuznetsov A, Lopez JP, Kash S, Ammala CE, Philipson LH. Kv2.1 ablation alters glucose-induced islet electrical activity, enhancing insulin secretion. Cell Metab. 2007; 6(3):229–235. [PubMed: 17767909]

Jenkins SM, Bennett V. Ankyrin-G coordinates assembly of the spectrin-based membrane skeleton, voltage-gated sodium channels, and L1 CAMs at Purkinje neuron initial segments. J Cell Biol. 2001; 155(5):739–746. [PubMed: 11724816]

Khirug S, Yamada J, Afzalov R, Voipio J, Khiroug L, Kaila K. GABAergic depolarization of the axon initial segment in cortical principal neurons is caused by the Na-K-2Cl cotransporter NKCC1. J Neurosci. 2008; 28(18):4635–4639. [PubMed: 18448640]

Klinger F, Gould G, Boehm S, Shapiro MS. Distribution of M-channel subunits KCNQ2 and KCNQ3 in rat hippocampus. NeuroImage. 2011; 58(3):761–769. [PubMed: 21787867]

Kole MH, Stuart GJ. Signal processing in the axon initial segment. Neuron. 2012; 73(2):235–247. [PubMed: 22284179]

Kosaka T. The axon initial segment as a synaptic site: ultrastructure and synaptology of the initial segment of the pyramidal cell in the rat hippocampus (CA3 region). J Neurocytol. 1980; 9(6):861–882. [PubMed: 7205337]

Lemaillet G, Walker B, Lambert S. Identification of a conserved ankyrin-binding motif in the family of sodium channel {alpha} subunits. J Biol Chem. 2003; 278(30):27333–27339. [PubMed: 12716895]

Lim ST, Antonucci DE, Scannevin RH, Trimmer JS. A novel targeting signal for proximal clustering of the Kv2.1 K+ channel in hippocampal neurons. Neuron. 2000; 25(2):385–397. [PubMed: 10719893]

Lorincz A, Nusser Z. Cell-type-dependent molecular composition of the axon initial segment. J Neurosci. 2008; 28(53):14329–14340. [PubMed: 19118165]

Manning CF, Bundros AM, Trimmer JS. Benefits and pitfalls of secondary antibodies: why choosing the right secondary is of primary importance. PLoS One. 2012; 7(6):e38313. [PubMed: 22675541]

Misonou H, Menegola M, Mohapatra DP, Guy LK, Park KS, Trimmer JS. Bidirectional activity-dependent regulation of neuronal ion channel phosphorylation. J Neurosci. 2006; 26(52):13505–13514. [PubMed: 17192433]

Misonou H, Mohapatra DP, Menegola M, Trimmer JS. Calcium- and metabolic state-dependent modulation of the voltage-dependent Kv2.1 channel regulates neuronal excitability in response to ischemia. J Neurosci. 2005; 25(48):11184–11193. [PubMed: 16319318]

Misonou H, Mohapatra DP, Park EW, Leung V, Zhen D, Misonou K, Anderson AE, Trimmer JS. Regulation of ion channel localization and phosphorylation by neuronal activity. Nat Neurosci. 2004; 7(7):711–718. [PubMed: 15195093]

Mohapatra DP, Misonou H, Pan SJ, Held JE, Surmeier DJ, Trimmer JS. Regulation of intrinsic excitability in hippocampal neurons by activity-dependent modulation of the KV2.1 potassium channel. Channels (Austin). 2009; 3(1):46–56. [PubMed: 19276663]

Mundel P, Gilbert P, Kriz W. Podocytes in glomerulus of rat kidney express a characteristic 44 KD protein. J Histochem Cytochem. 1991; 39(8):1047–1056. [PubMed: 1856454]

O'Connell KM, Rolig AS, Whitesell JD, Tamkun MM. Kv2.1 potassium channels are retained within dynamic cell surface microdomains that are defined by a perimeter fence. J Neurosci. 2006; 26(38):9609–9618. [PubMed: 16988031]

Ogawa Y, Horresh I, Trimmer JS, Bredt DS, Peles E, Rasband MN. Postsynaptic density-93 clusters Kv1 channels at axon initial segments independently of Caspr2. J Neurosci. 2008; 28(22):5731–5739. [PubMed: 18509034]

Pan Z, Kao T, Horvath Z, Lemos J, Sul JY, Cranstoun SD, Bennett V, Scherer SS, Cooper EC. A common ankyrin-G-based mechanism retains KCNQ and NaV channels at electrically active domains of the axon. J Neurosci. 2006; 26(10):2599–2613. [PubMed: 16525039]

Park KS, Mohapatra DP, Misonou H, Trimmer JS. Graded regulation of the Kv2.1 potassium channel by variable phosphorylation. Science. 2006; 313(5789):976–979. [PubMed: 16917065]

Plant LD, Dowdell EJ, Dementieva IS, Marks JD, Goldstein SA. SUMO modification of cell surface Kv2.1 potassium channels regulates the activity of rat hippocampal neurons. J Gen Physiol. 2011; 137(5):441–454. [PubMed: 21518833]

Racine R, Okujava V, Chipashvili S. Modification of seizure activity by electrical stimulation. 3. Mechanisms. Electroencephalogr Clin Neurophysiol. 1972; 32(3):295–299. [PubMed: 4110398]

Rasband MN. Composition, assembly, and maintenance of excitable membrane domains in myelinated axons. Semin Cell Dev Biol. 2011; 22(2):178–184. [PubMed: 20932927]

Rasmussen HB, Frokjaer-Jensen C, Jensen CS, Jensen HS, Jorgensen NK, Misonou H, Trimmer JS, Olesen SP, Schmitt N. Requirement of subunit co-assembly and ankyrin-G for M-channel localization at the axon initial segment. J Cell Sci. 2007; 120(Pt 6):953–963. [PubMed: 17311847]

Saliba RS, Kretschmannova K, Moss SJ. Activity-dependent phosphorylation of GABAA receptors regulates receptor insertion and tonic current. EMBO J. 2012; 31(13):2937–2951. [PubMed: 22531784]

Sanchez-Ponce D, Blazquez-Llorca L, DeFelipe J, Garrido JJ, Munoz A. Colocalization of alpha-actinin and synaptopodin in the pyramidal cell axon initial segment. Cereb Cortex. 2012; 22(7): 1648–1661. [PubMed: 21940706]

Sarmiere PD, Weigle CM, Tamkun MM. The Kv2.1 K+ channel targets to the axon initial segment of hippocampal and cortical neurons in culture and in situ. BMC Neurosci. 2008; 9:112. [PubMed: 19014551]

Scannevin RH, Murakoshi H, Rhodes KJ, Trimmer JS. Identification of a cytoplasmic domain important in the polarized expression and clustering of the Kv2.1 K+ channel. J Cell Biol. 1996; 135(6 Pt 1):1619–1632. [PubMed: 8978827]

Schafer DP, Jha S, Liu F, Akella T, McCullough LD, Rasband MN. Disruption of the axon initial segment cytoskeleton is a new mechanism for neuronal injury. J Neurosci. 2009; 29(42):13242–13254. [PubMed: 19846712]

Sobotzik JM, Sie JM, Politi C, Del Turco D, Bennett V, Deller T, Schultz C. AnkyrinG is required to maintain axo-dendritic polarity in vivo. Proc Natl Acad Sci U S A. 2009; 106(41):17564–17569. [PubMed: 19805144]

Song AH, Wang D, Chen G, Li Y, Luo J, Duan S, Poo MM. A selective filter for cytoplasmic transport at the axon initial segment. Cell. 2009; 136(6):1148–1160. [PubMed: 19268344]

Szabadics J, Varga C, Molnar G, Olah S, Barzo P, Tamas G. Excitatory effect of GABAergic axo-axonic cells in cortical microcircuits. Science. 2006; 311(5758):233–235. [PubMed: 16410524]

Szu-Yu Ho T, Rasband MN. Maintenance of neuronal polarity. Dev Neurobiol. 2011; 71(6):474–482. [PubMed: 21557501]

Tamkun MM, O'Connell KM, Rolig AS. A cytoskeletal-based perimeter fence selectively corrals a sub-population of cell surface Kv2.1 channels. J Cell Sci. 2007; 120(Pt 14):2413–2423. [PubMed: 17606996]

Trimmer JS. Immunological identification and characterization of a delayed rectifier K+ channel polypeptide in rat brain. Proc Natl Acad Sci U S A. 1991; 88(23):10764–10768. [PubMed: 1961744]

Trimmer, JS.; Misonou, H. Phosphorylation of voltage-gated ion channels. In: Zheng, J.; Trudeau, MC., editors. Handbook of Ion Channels. Boca Raton, FL: CRC Press; 2014.

Vacher H, Trimmer JS. Trafficking mechanisms underlying neuronal voltage-gated ion channel localization at the axon initial segment. Epilepsia. 2012; 53(Suppl 9):21–31. [PubMed: 23216576]

Van Wart A, Trimmer JS, Matthews G. Polarized distribution of ion channels within microdomains of the axon initial segment. J Comp Neurol. 2007; 500(2):339–352. [PubMed: 17111377]

Vlachos A, Ikenberg B, Lenz M, Becker D, Reifenberg K, Bas-Orth C, Deller T. Synaptopodin regulates denervation-induced homeostatic synaptic plasticity. Proc Natl Acad Sci U S A. 2013; 110(20):8242–8247. [PubMed: 23630268]

Vlachos A, Korkotian E, Schonfeld E, Copanaki E, Deller T, Segal M. Synaptopodin regulates plasticity of dendritic spines in hippocampal neurons. J Neurosci. 2009; 29(4):1017–1033. [PubMed: 19176811]

Watanabe K, Al-Bassam S, Miyazaki Y, Wandless TJ, Webster P, Arnold DB. Networks of polarized actin filaments in the axon initial segment provide a mechanism for sorting axonal and dendritic proteins. Cell Rep. 2012; 2(6):1546–1553. [PubMed: 23246006]

Wimmer VC, Reid CA, So EY, Berkovic SF, Petrou S. Axon initial segment dysfunction in epilepsy. J Physiol. 2010; 588(Pt 11):1829–1840. [PubMed: 20375142]

Winckler B, Forscher P, Mellman I. A diffusion barrier maintains distribution of membrane proteins in polarized neurons. Nature. 1999; 397(6721):698–701. [PubMed: 10067893]

Woodruff AR, Anderson SA, Yuste R. The enigmatic function of chandelier cells. Front Neurosci. 2010; 4:201. [PubMed: 21151823]

Wyszynski M, Kharazia V, Shanghvi R, Rao A, Beggs AH, Craig AM, Weinberg R, Sheng M. Differential regional expression and ultrastructural localization of alpha-actinin-2, a putative NMDA receptor-anchoring protein, in rat brain. J Neurosci. 1998; 18(4):1383–1392. [PubMed: 9454847]

Xiao M, Bosch MK, Nerbonne JM, Ornitz DM. FGF14 localization and organization of the axon initial segment. Mol Cell Neurosci. 2013; 56:393–403. [PubMed: 23891806]

Zhang XL, Poschel B, Faul C, Upreti C, Stanton PK, Mundel P. Essential role for synaptopodin in dendritic spine plasticity of the developing hippocampus. J Neurosci. 2013; 33(30):12510–12518. [PubMed: 23884954]

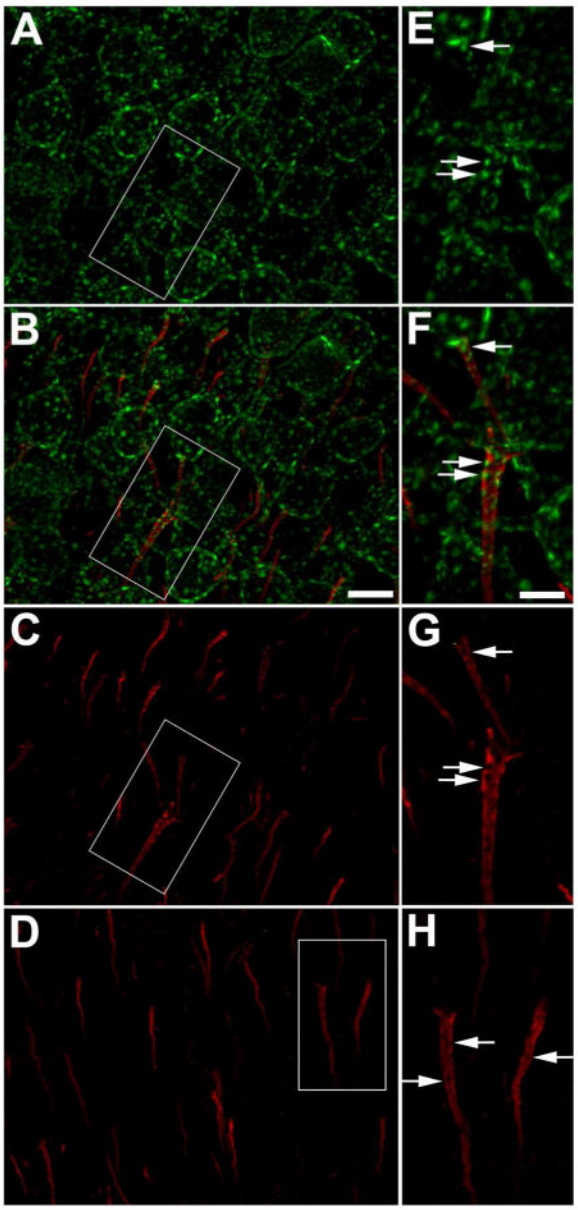

Figure 1.

Kv2.1 is localized on the AIS of mouse neocortical neurons. A-D: Mouse brain sections double immunofluorescence labeled for Kv2.1 (green) and AnkG (red). Panels E-H are 2X-magnified images of boxed regions on panels A-D, respectively. Panels AC: WT mouse brain section. Arrows in panels E-G correspond to same locations on each panel. A: Images of Kv2.1 labeling alone. Note prominent localization of Kv2.1 in large clusters on neuronal somata and proximal dendrites. B: Images of double immunofluorescence labeling for Kv2.1 (red) and AnkG. Note prominent clustered localization of Kv2.1 clusters on the AIS (arrows) as revealed by the AnkG labeling. C: Images of AnkG labeling alone. Note that the sites of Kv2.1 clustering on the AIS (arrows) seen in panels A and B occur at sites deficient in AnkG. D: $Kv2.1^{-/-}$ mouse brain section. Note lack of Kv2.1 labeling in $Kv2.1^{-/-}$ brain, and persistence of AnkG-deficient sites on the AIS (arrows). Scale bar on panel B for panels A-

D: 10 μm; scale bar on panel F for panels E-H: 5 μm (2X magnified). All images were obtained using Apotome structured illumination microscopy. A magenta-green version of this figure is available online as Supplementary Figure 1.

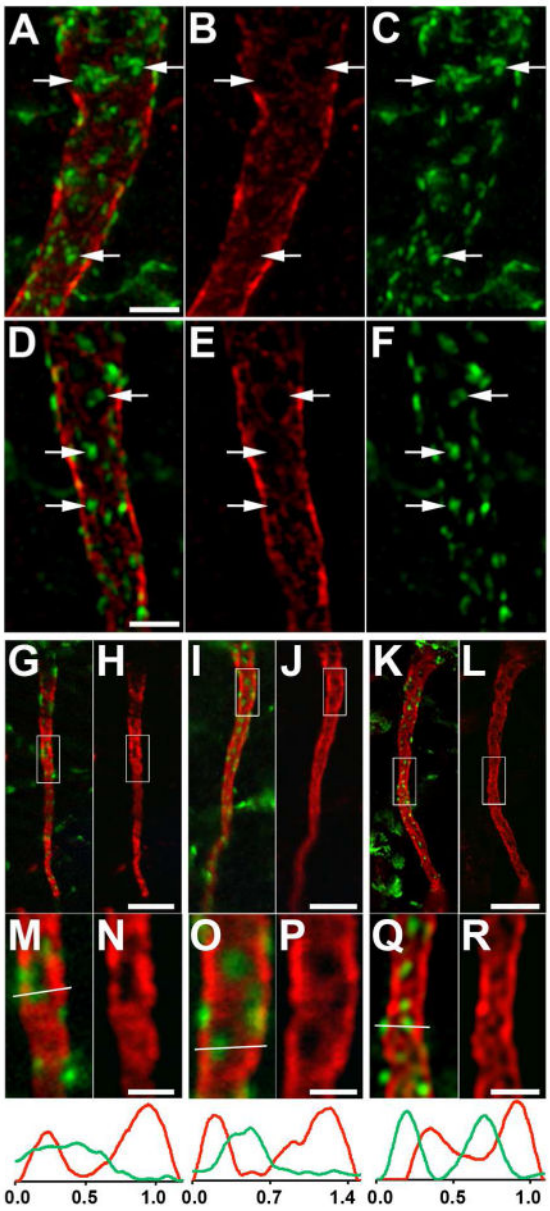

Figure 2.

Kv2.1 is localized at AnkG-deficient sites on the AIS of rat layer 5 neocortical pyramidal neurons. Rat brain sections double immunofluorescence labeled for Kv2.1 (green) and AnkG (red). A-F: Images obtained with a Zeiss Elyra super resolution microscope, showing two examples (A-C and D-F) of double labeling (A,D), and the AnkG (B,E) and Kv2.1 (C,F) signals alone. Arrows in panels correspond to same locations on each panel. G-R: Images showing double labeling (G,I,K), and the AnkG signal alone (H,J,L). G,H: Images obtained with a Zeiss Apotome microscope. I,J: Images obtained with an Olympus confocal microscope. K,L: Images obtained with a Nikon N-SIM microscope. Panels below M-R are 4X-magnified images of the area shown in the boxes in panels G-L above. Graphs below panels M-R are histograms of fluorescence intensity across the line drawn on each panel. Scale bar on panel D for panels A-F: 2 μm. Scale bar on panel H for panels G-L: 5 μm. Scale

bar on panel H for panels G,H, on panel J for panels I,J, on panel L for panels K,L; on panel N for panels M,N, on panel P for panels O,P, and on panel R for panels Q,R: 1.25 μm. A magenta-green version of this figure is available online as Supplementary Figure 2.

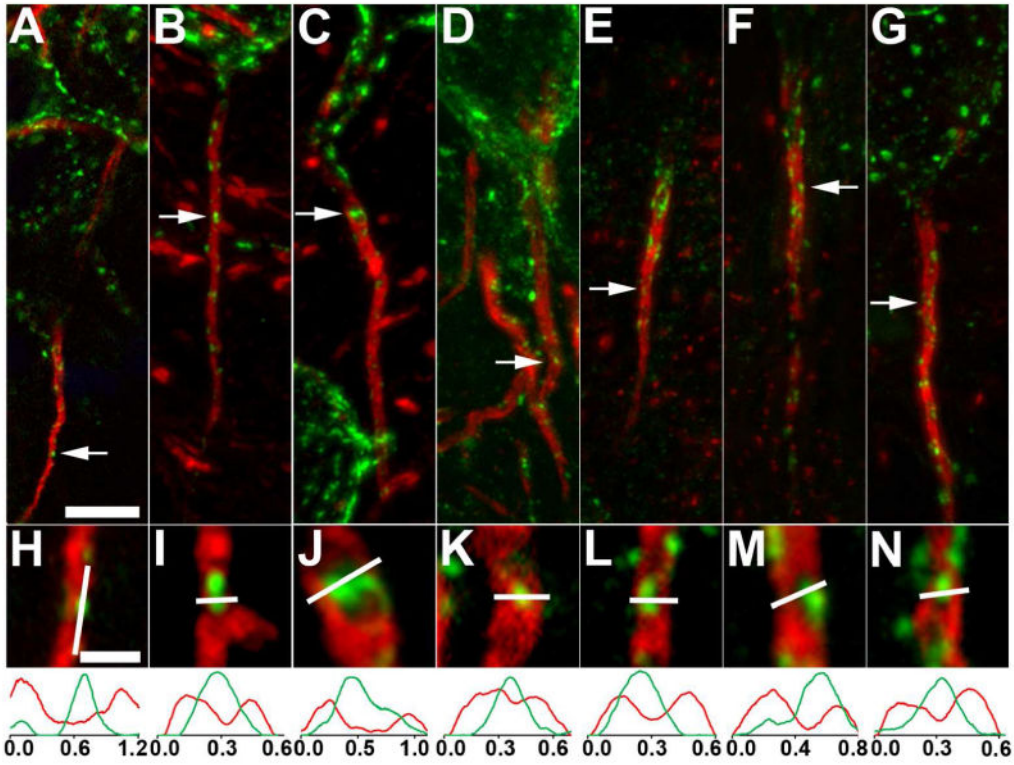

Figure 3.

Kv2.1 is localized at AnkG-deficient sites on the AIS of neurons in different regions of rat brain. Rat brain sections double immunofluorescence labeled for Kv2.1 (green) and AnkG (red). Images were obtained from neurons in different brain regions. A-D, H-K: hippocampus. A,H: CA1 pyramidal neurons; B,I: a parvalbumin-negative interneuron in *stratum oriens* of CA1; C,J: a parvalbumin-positive interneuron in *stratum oriens* of CA1; D,K: dentate granule cells. E,F,L,M: thalamus. E,L: a neuron in the posterior nucleus; F,M: a neuron in the lateral posterior nucleus. G,N: a medium spiny neuron in the striatum. Arrows in panels correspond to the location of the midpoint of the 4X enlarged insets in panels H-N. Graphs below panels H-N are histograms of fluorescence intensity across the line drawn on each panel. Scale bar on panel A for panels A-G: 5 μm; Scale bar on panel H for panels H-N: 1 μm (4X magnified). All images were obtained using Apotome structured illumination microscopy. A magenta-green version of this figure is available online as Supplementary Figure 3.

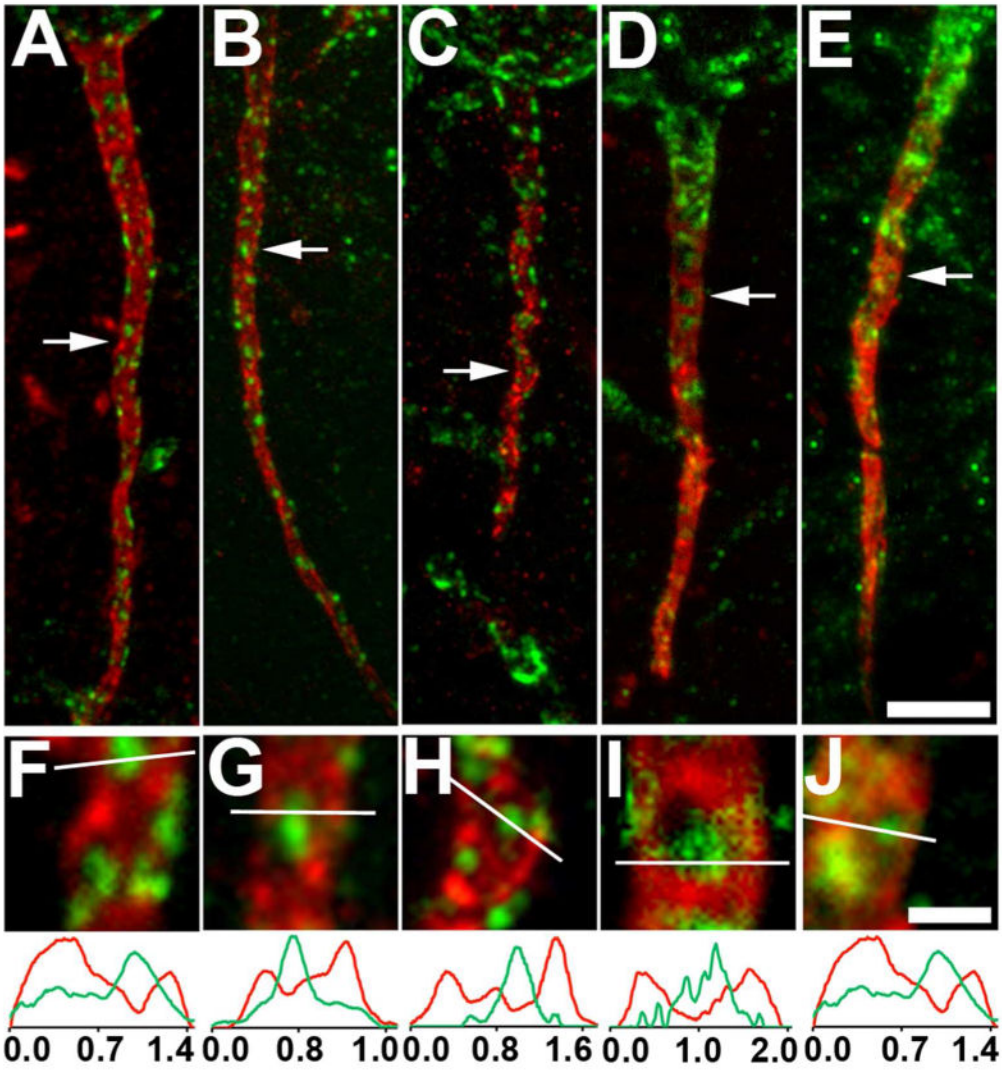

Figure 4.

Kv2.1 is localized at AnkG-deficient sites on the AIS of layer 5 neocortical pyramidal neurons in different mammalian species. Sections double immunofluorescence labeled for Kv2.1 (green) and AnkG (red). Images were obtained from neocortical neurons in the brains of different mammalian species: A,F: rat; B,G: ferret; C,H: monkey; D,E,I,J: human. Arrows in panels A-E correspond to the location of the midpoint of the 4X enlarged insets shown as panels F-J, respectively. Graphs below panels F-J are histograms of fluorescence intensity across the line drawn on each panel. Scale bar on panel E for panels A-E: 5 μm; Scale bar on panel J for panels F-J: 1 μm (4X magnified). All images were obtained using Apotome structured illumination microscopy. A magenta-green version of this figure is available online as Supplementary Figure 4.

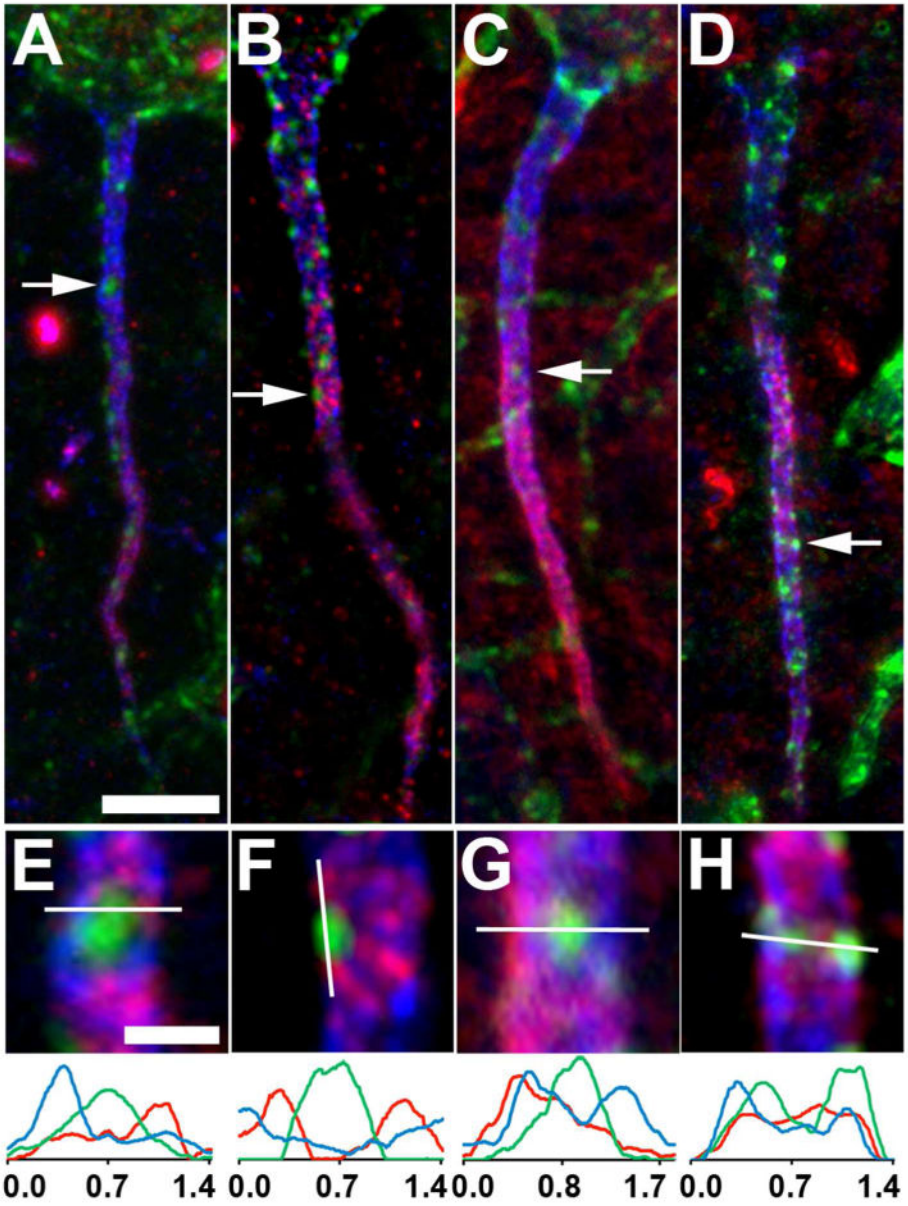

Figure 5.

Kv2.1 localization relative to other voltage-gated ion channels on the AIS of layer 5 neocortical pyramidal neurons. Triple immunofluorescence labeling for Kv2.1 (green), AnkG (blue) and in red, either Nav1.6 (A,B,E,F) or Kv1.2 (C,D,G,H). Panels A,C,E,G were obtained using Apotome structured illumination microscopy, panels B,D,F,H were obtained using N-Sim super resolution structured illumination microscopy. Arrows in panels A-D correspond to the location of the midpoint of the 4X enlarged insets in panels E-H, respectively. Note that the bright spot in the Nav1.6 panel A just below the arrow is likely a node of Ranvier of a myelinated axon. Graphs below magnified insets E-H are histograms of fluorescence intensity across the line drawn on each panel. Scale bar on panel A for panels A-D: 5 μm; Scale bar on panel E for panels E-H: 1 μm (4X magnified).

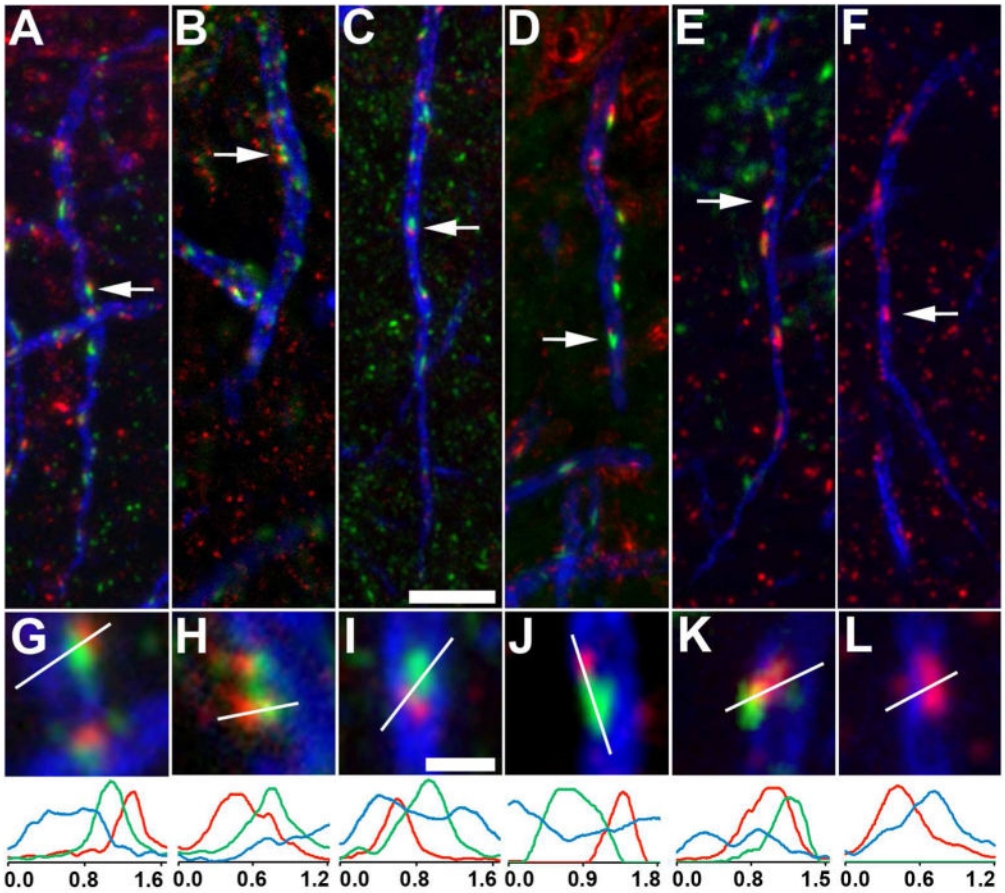

Figure 6.

Kv2.1 is localized adjacent to components of the cisternal organelle (CO) complex on the AIS of layer 5 neocortical pyramidal neurons. Triple immunofluorescence labeling for Kv2.1 (green), AnkG (blue) and in red, components of the CO complex. All panels are from rat neocortex with the exception of panels E, F, K, L, which are from neocortex of wild-type (E,K) and *Kv2.1*$^{-/-}$ (F, L) mouse littermates. A,G, E-L: synaptopodin; B,H: ryanodine receptor intracellular calcium release channel; C,I: α-actinin; D,J: F-actin. Arrows in panels A-F correspond to the location of the midpoint of the 4X enlarged insets in panels G-L. Graphs below magnified insets are histograms of fluorescence intensity across the line drawn on each panel G-L. Scale bar on panel C for panels A-F: 5 μm; Scale bar on panel I for panels G-L: 1 μm (4X magnified). All images were obtained using Apotome structured illumination microscopy.

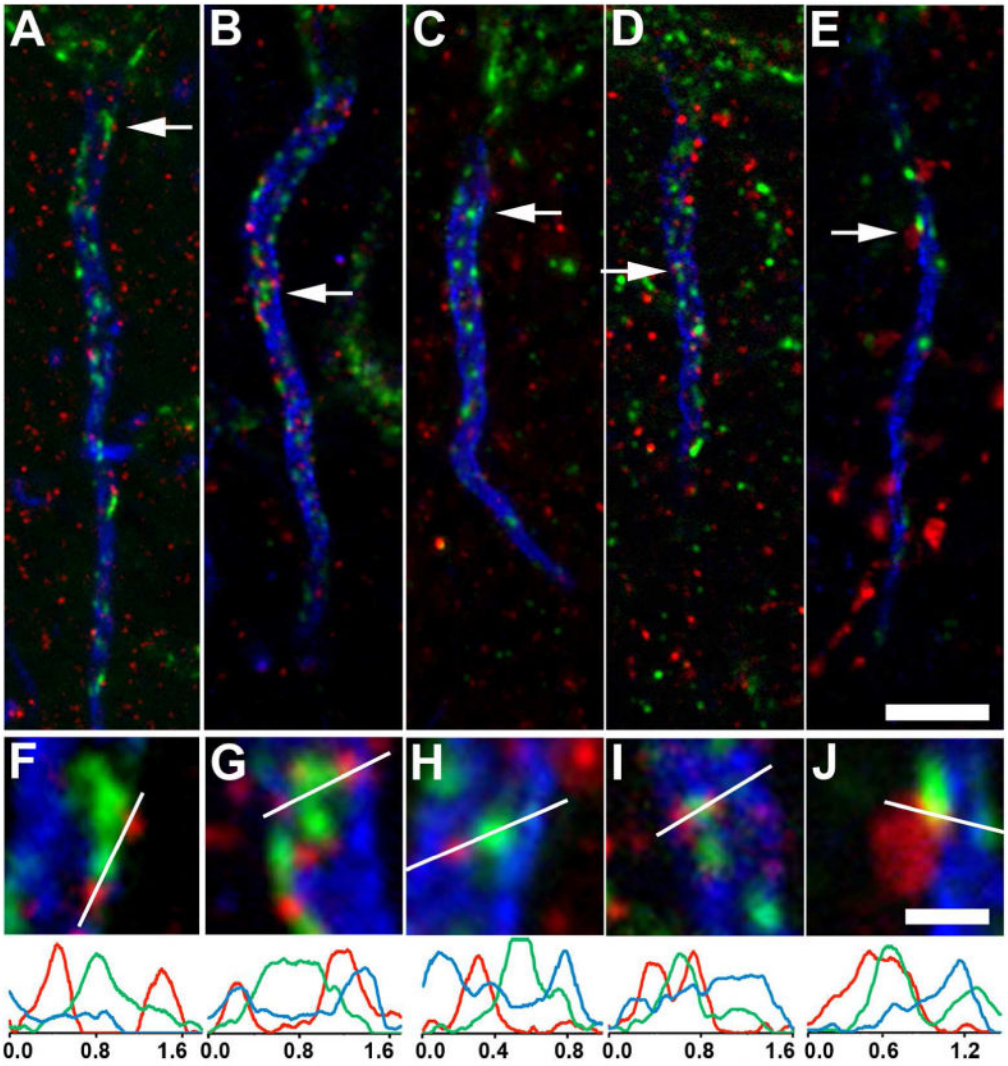

Figure 7.

Kv2.1 is localized adjacent to components of GABA-A receptor complexes on the AIS of rat layer 5 neocortical pyramidal neurons. Triple immunofluorescence labeling for Kv2.1 (green), AnkG (blue) and in red, components of GABA-A receptor synapses. A,F: α1 subunit; B,G: β1 subunit; C,H: β3 subunit; D,I: gephyrin; E,J: vesicular GABA transporter. Arrows in panels A-E correspond to the location of the midpoint of the 4X enlarged insets in panels F-J, respectively. Graphs below magnified insets are histograms of fluorescence intensity across the line drawn on each panel F-L. Scale bars: Scale bar on panel E for panels A-E: 5 μm; Scale bar on panel J for panels F-J: 1 μm (4X magnified). All images were obtained using Apotome structured illumination microscopy.

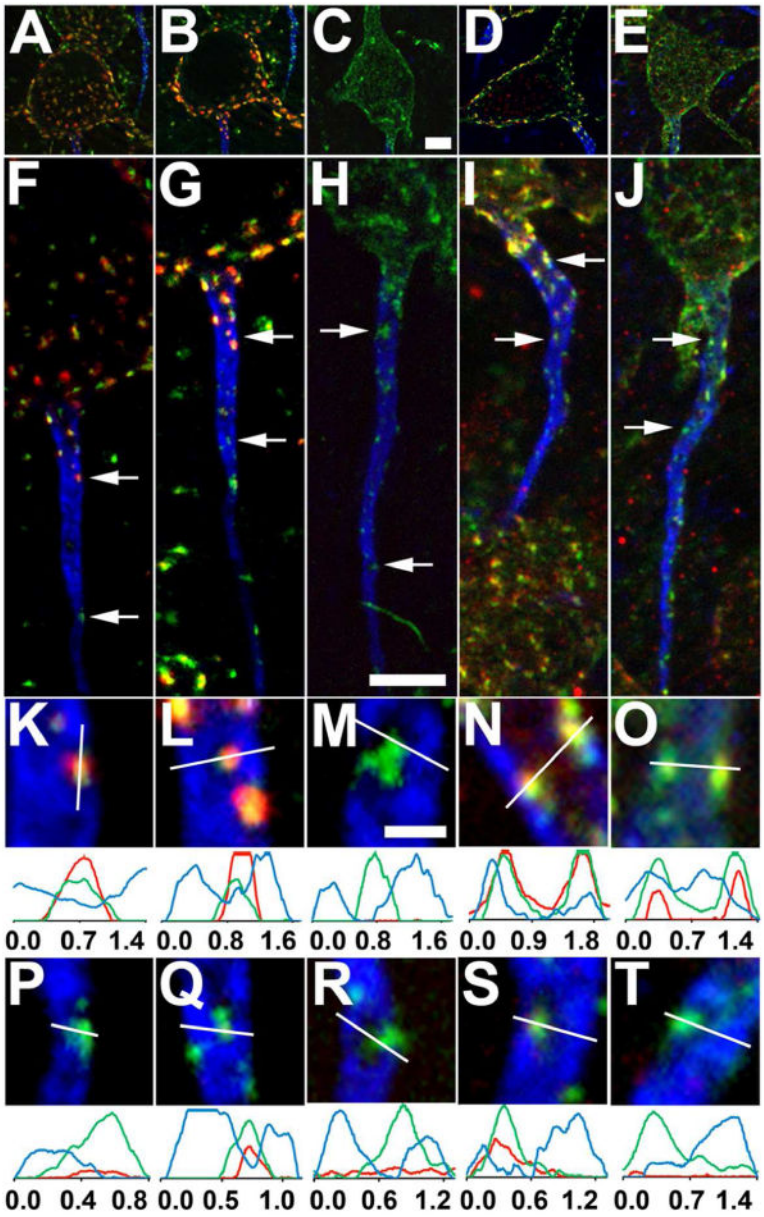

Figure 8.

Kv2.1 phosphorylation state differs on the proximal and distal AIS of rat layer 5 neocortical pyramidal neurons. Triple immunofluorescence labeling for Kv2.1 (green), AnkG (blue) and in red, Kv2.1 phosphorylated at S603. Sections were prepared from either saline injected rats (panels A,F,K,P and panels B,G,L,Q), or from rats subjected to seizures in response to kainate injection (C,H,M,R). Alternatively, sections were prepared from control rats (D,I,N,S), or rats subjected to brief CO_2-induced hypoxia (E,J,O,T). Panels A-E are low magnification (4X reduced) images of somata corresponding to the AIS shown below. Arrows in panels F-J correspond to the location of the midpoint of the 4X enlarged insets in panels K-T, taken from proximal (panels K-O) or distal (panels P-T) regions of the AIS. Graphs below magnified insets are histograms of fluorescence intensity across the line

drawn on each panel. Scale bar on panel C for panels A-E, and on panel H for panels F-J: 5 μm; Scale bar on panel M for panels K-T: 1 μm (4X magnified). All images were obtained using Apotome structured illumination microscopy.

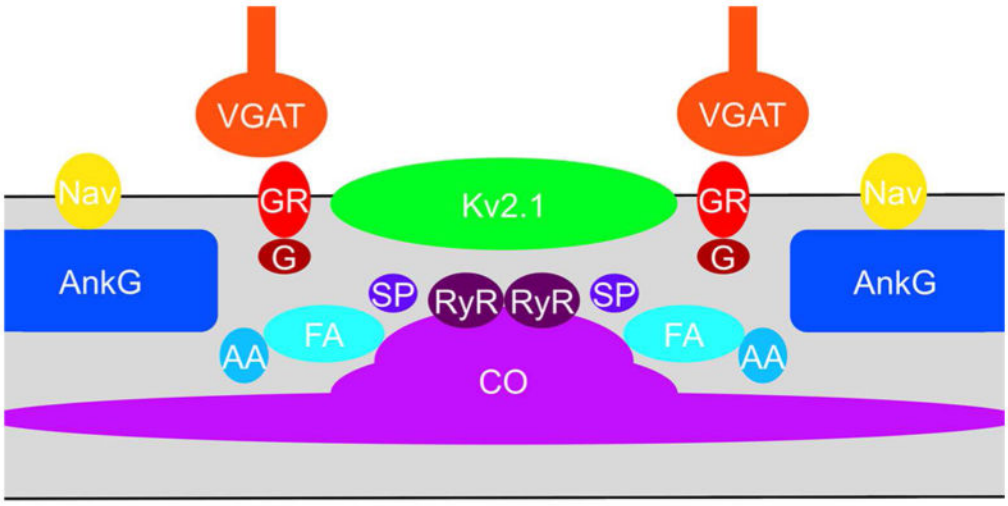

Figure 9.

Schematic of components of AnkG-deficient sites on the AIS. Components identified in this study as exhibiting localization at AnkG-deficient sites on the AIS. AA: α-actinin; CO; cisternal organelle; FA: F-actin; G: gephyrin; GR: GABA-A receptor; Nav: Nav channel; RyR: ryanodine receptor; SP: synaptopodin.

Table 1

Antibodies used in this study

Target	Host	Type	Clone/Name	Immunogen	Source	Catalog #	Form	Conc/dilution	Isotype
Kv2.1	Mouse	Mono	K89/34	a.a. 837-853 rat HMLPGGGAHGSTRDQSI	NeuroMab	75-014	Purified IgG	10 ug/mL	IgG1
Kv2.1	Rabbit	Poly	KC	a.a. 837-853 rat HMLPGGGAHGSTRDQSI	Trimmer lab	NA	Affinity-Purified	1:100	

Target	Host	Type	Clone/Name	Immunogen	Source	Catalog #	Form	Concdilution	Isotype
Ankyrin-G	Mouse	Mono	N106/36	full length human EDAMTGDTDKYLG PQDLKELGDDSLP AEGYMGFSLGARS ASLRSFSSDRSYTL NRSSYARDSMMIE ELLVPSKEQHLTFT REFDSDSLRHYSW AADTLDNVNLVSS PIHSGFLVSFMVDA RGGSMRGSRHHG MRIIIPPRKCTAPTR ITCRLVKRHKLANP PPMVEGEGLASRL VEMGPAGAQFLGP VIVEIPHFGSMRGK ERELIVLRSENGET WKEHQFDSKNEDL TELLNGMDEELDS PEELGKKRICRIITK DFPQYFAVVSRIKQ ESNQIGPEGGILSS TTVPLVQASFPEG ALTKRIRVGLQAQP VPDEIVKKILGNKA TFSPIVTVEPRRRK FHKPITMTIPVPPP SGEGVSNGYKGDT TPNLRLLCSITGGT SPAQWEDITGTTPL TFIKDCVSFTTNVS ARFWLADCHQVLE TVGLATQLYRELIC VPYMAKFVVFAKM NDPVESSLRCFCM TDDKVDKTLEQQE NFEEVARSKDIEVL EGKPIYVDCYGNLA PLTKGGQQLVFNF YSFKENRLPFSIKIR DTSQEPCCGRLSFL KEPKTTKGLPQTA VCNLNITLPAHKKIE KTDRRQSFASLAL RKRYSYLTEPGMS PQSPCERTDIRMAI VADHLGLSWTELA RELNFSVDEINQIR VENPNSLISQSFML LKKWVTRDGKNAT TDALTSVLTKINRID IVTLLEGPIFDYGNI SGTRSFADENNVF HDPVDDGPPVVTA EDASLEDSKLEDS VPLTEMPEAVDVD ESQLENVCLSWQN ETSSGNLESCAQA RRVTGGLLDRLDD SPDQCRDSITSYLK GEAGKFEANGSHT EITPEAKTKSYFPE SQNDVGKQSTKET LKPKIHGSGHVEEP ASPLAAYQKSLEET SKLIEETKPCVPVS	NeuroMab	75-146	Purified IgG	10 ug/mL	IgG2a

Target	Host	Type	Clone/Name	Immunogen	Source	Catalog #	Form	Concdilution	Isotype
Ankyrin-G	Mouse	Mono	N106/65	full length human EDAMTGDTDKYLG PQDLKELGDDSLP AEGYMGFSLGARS ASLRSFSSDRSYTL NRSSYARDSMMIE ELLVPSKEQHLTFT REFDSDSLRHYSW AADTLDNVNLVSS PIHSGFLVSFMVDA RGGSMRGSRHHG MRIIIPPRKCTAPTR ITCRLVKRHKLANP PPMVEGEGLASRL VEMGPAGAQFLGP VIVEIPHFGSMRGK ERELIVLRSENGET WKEHQFDSKNEDL TELLNGMDEELDS PEELGKKRICRIITK DFPQYFAVVSRIKQ ESNQIGPEGGILSS TTVPLVQASFPEG ALTKRIRVGLQAQP VPDEIVKKILGNKA TFSPIVTVEPRRRK FHKPITMTIPVPPP SGEGVSNGYKGDT TPNLRLLCSITGGT SPAQWEDITGTTPL TFIKDCVSFTTNVS ARFWLADCHQVLE TVGLATQLYRELIC VPYMAKFVVFAKM NDPVESSLRCFCM TDDKVDKTLEQQE NFEEVARSKDIEVL EGKPIYVDCYGNLA PLTKGGQQLVFNF YSFKENRLPFSIKIR DTSQEPCCGRLSFL KEPKTTKGLPQTA VCNLNITLPAHKKIE KTDRRQSFASLAL RKRYSYLTEPGMS PQSPCERTDIRMAI VADHLGLSWTELA RELNFSVDEINQIR VENPNSLISQSFML LKKWVTRDGKNAT TDALTSVLTKINRID IVTLLEGPIFDYGNI SGTRSFADENNVF HDPVDDGPPVVTA EDASLEDSKLEDS VPLTEMPEAVDVD ESQLENVCLSWQN ETSSGNLESCAQA RRVTGGLLDRLDD SPDQCRDSITSYLK GEAGKFEANGSHT EITPEAKTKSYFPE SQNDVGKQSTKET LKPKIHGSGHVEEP ASPLAAYQKSLEET SKLIIEETKPCVPVS	NeuroMab	75-147	Purified IgG	10 ug/mL	IgG2b

Target	Host	Type	Clone/Name	Immunogen	Source	Catalog #	Form	Conc/dilution	Isotype
Parvalbumin	Rabbit	Poly		full length rat MSMTDLLSAEDIKKAI GAFTAADSFDHKKFF QMVGLKKKSADDVK KVFHILDKDKSGFIEE DELGSILKGFSSDAR DLSAKETKTLMAAGD KDGDGKIGVEEFSTL VAES	Abcam	Ab11427	Affinity-Purified	11 ug/mL	
Kv1.2	Mouse	Mono	K14/16	a.a. 428-499 rat QYLQVTSCPKIPSSP DLKKSRSASTISKSD YMEIQEGVNNSNEDF REENLKTANCTLANT NYVNITKMLTDV	NeuroMab	75-008	Purified IgG	10 ug/mL	IgG2b
Nav1.6	Mouse	Mono	K87A/10	a.a. 459-476 rat SEDAIEEEGEDGVGS PRS	NeuroMab	75-026	Purified IgG	10 ug/mL	IgG1
Synaptopodin	Mouse	Mono	G1D4	Isolated rat kidney glomeruli	Acris	BM5086	TC supe	1:100	IgG1
Ryanodine Receptor	Mouse	Mono	34C	purified chicken muscle ryanodine receptor	Pierce	MA3-925	Purified IgG	1 ug/mL	IgG1
α-actinin	Mouse	Mono	EA-53	purified rabbit skeletal α actinin	Sigma-Aldrich	A7732	Purified IgG	10 ug/mL	IgG1
GABA(A) R α1	Mouse	Mono	N95/35	a.a. 355-394 human KKVKDPLIKKNNTYA PTATSYTPNLARGDP GLATIAKSAT	NeuroMab	75-136	TC supe	1:5	IgG2a
GABA(A) R β1	Mouse	Mono	N96/55	a.a. 327-450 mouse VNYIFFGKGPQKKGA SKQDQSANEKNRLE MNKVQVDAHGNILLS TLEIRNETSGSEVLT GVSDPKATMYSYDS ASIQYRKPLSSREGF GRGLDRHGVPGKGR IRRRASQLKVKIPDLT DVNSID	NeuroMab	75-137	TC supe	1:5	IgG1
GABA(A) R β3	Mouse	Mono	N87/25	a.a. 370-433 mouse APMDVHNEMNEVAG SVGDTRNSAISFDNS GIQYRKQSMPKEGH GRYMGDRSIPHKKT HLRRRSS	NeuroMab	75-149	TC supe	1:5	IgG1
Gephyrin	Mouse	Mono	mAb7a (GlyR7a)	purified rat gephyrin	Synaptic Systems	147 011	Purified IgG	10 ug/mL	IgG1

Target	Host	Type	Clone/Name	Immunogen	Source	Catalog #	Form	Conc/dilution	Isotype
VGAT	Rabbit	Poly		a.a. 75-87 rat AEPPVEGDIHYQR	Synaptic Systems	131 003	Affinity-Purified	2 ug/mL	
Kv2.1 S603P	Rabbit	Poly	M1675	a.a. 596-616, p603 rat CEATRFSHpSPLASL SSKAGSST	Trimmer lab	NA	Antiserum	1:500	
Bodipy FL Phallacidin					Invitrogen	B607	toxin-dye conjugate	4 units/mL	